Research Article | Vol. 2, No. 3 / 15 March 2019 / OSA Continuum 923

Modulation format/bit rate recognition based on principal component analysis (PCA) and artificial neural networks (ANNs)

JUNHE ZHOU* AND PANPAN FAN

Dept. of Electronics Science and Engineering, Tongji University, Shanghai 200092, China
*jhzhou@tongji.edu.cn

Abstract: In this paper, we propose a novel approach to recognize modulation formats/bit rates. Firstly, the polarization multiplexed (pol-mux) signal is splitted by a polarization beam splitter (PBS) to generate asynchronous delay tap plots (ADTPs). The ADTP patterns are analyzed by principal component analysis (PCA), and the principal eigenvalues and the principal eigenvectors are evaluated. Afterwards, the ADTPs are converted into the weight vectors by projecting them onto the principal eigenvector directions. The weight vectors from the training signals are sent to train the artificial neural network (ANN) and the trained ANN can distinguish the modulation formats/bit rates of the detected signals by taking their weight vectors as the input. The proposed PCA + ANN method allows modulation format/bit rate recognition for 16 different types of data streams. 14 traditional modulate formats achieve 99% recognition accuracy with 20 dB OSNR, which is a significant improvement in comparison with the existing methods. 2 OFDM signals can also be distinguished with about 85% accuracy.

1. Introduction

Different modulation formats such as OOK, QPSK, 16QAM [1–3] etc. have been adopted in optical communication systems. In such heterogeneous optical networks, dynamic channel variations require the receivers to adapt to different modulation formats/bit rates. Hence, accurate modulation format/bit rate recognition is highly demanded.

Coherent data-aided modulation format/bit rate recognition [4–12] is rather accurate. These methods use the techniques like K-means algorithm [4], higher order cumulents analysis [5], power distribution [6] or peak to average power ratio (PAPR) analysis [7] at the coherent receiver side, Stokes space parameter analysis [8–9], pilot signal aided carrier phase recovery [10], frequency offset loading [11] and supported vector machines [12]. However, the introduction of the coherent receiver for optical monitoring significantly increases the system complexity. Therefore, direct detection based modulation format/bit rate recognition is still attractive in research and development.

The direct analysis of the signal power characteristics, such as power distribution [6] can help to distinguish the different modulation formats, however, it is not possible identify the different bit rates. To overcome this, several efficient direct detection based modulation format/bit rate recognition methods were proposed, such as asynchronous delay tap plots (ADTPs), asynchronous amplitude histograms (AAHs), etc. All these methods collect the signal power data, and their analyses are usually based on the pattern recognition methods, such as principal component analysis (PCA) [13–14] and artificial neural networks (ANNs) [15–16] etc. These methods achieve quite accurate recognition results [13–16]. Particularly the ANN based approach can be trained to automatically recognize the main features of the signal modulate formats/bit rates, without any further prior information. However, ANN may encounter the problem of over fitting and fail to recognize the correct modulation formats/bit rates when the number of signal types is large. Currently, the number of different supported modulation formats/bit rates remains below

#343075 https://doi.org/10.1364/OSAC.2.000923
Journal © 2019 Received 23 Aug 2018; accepted 19 Feb 2019; published 13 Mar 2019

OSA CONTINUUM

ten (six in [13], three in [14], six in [15] and six in [16]). In addition to that, there is still potential to further improve the identification error rate. Therefore, it is necessary to look for a new method to distinguish more modulation formats/bit rates in a more robust and accurate way and resolve the problem of over fitting if ANN is implemented, despite the outstanding pioneering works on this topic [4–16].

In this paper, we propose a new method for modulation format/bit rate recognition. The signal passes through a polarization beam splitter to be separated into its x and y polarization components. Such an arrangement eases distinguishing between the pol-mux signal and the non-pol-mux signal formats. Afterwards, the two signal components along with the overall signal are used to generate ADTPs, which are analyzed by PCA, and the principal eigenvalues and the principal eigenvectors are collected. By implementing PCA, the main features to characterize the signal types are more significant and one may avoid the problem of over fitting for the ANN in the next step. The training signals have their ADTP vectors projected onto the principal eigenvector directions and the corresponding weight vectors are used to train an ANN. The trained ANN can recognize the signal modulation formats/bit rates by taking the weight vector of the detected signals as the input. The results show that our method improves the performance significantly in comparison with the existing approaches.

2. Methods

In this section, we will introduce the new recognition method in detail.

First of all, the signal, which might be pol-muxed, is splitted by the polarization beam splitter. Each of the polarization components along with the overall signal will be used for the ADTP generation [13,17]. The corresponding signal model to generate the ADTPs is:

$$\begin{aligned} a_{nx} &= |E_x(nT)|^2 \\ b_{nx} &= |E_x(nT - \Delta T)|^2 \\ a_{ny} &= |E_y(nT)|^2 \\ b_{ny} &= |E_y(nT - \Delta T)|^2 \\ c_n &= a_{nx} + a_{ny} \\ d_n &= b_{nx} + b_{ny} \end{aligned} \tag{1}$$

where T is the sampling period, ΔT the delay between the two consecutive streams to generate the ADTPs, a_{nx}, a_{ny}, b_{nx}, and b_{ny} stand for the corresponding asynchronous delay tap samples (ADTS) in the x and y polarization directions, and each pair of (a_{ni}, b_{ni}) (i = x,y) can be used to generate one ADTP. a_{nx}, a_{ny}, b_{nx}, and b_{ny} can be combined to get (c_{n}, d_{n}), which can be used to create the conventional ADTP [13,17].

ADTPs are generated by obtaining the two-dimensional histograms with respect to the pairs. In Fig. 1, the ADTPs generated by the pairs (c_{n}, d_{n}) of the 16 signals with different modulation formats/bit rates are shown. Similarly, we can have 32 more ADTPs based on the pairs (a_{ni}, b_{ni}) (i = x,y).

Several parameters will impact the ADTP patterns, such as the time delay ΔT between the two consecutive symbol pairs, the data format, the data baud rate, and whether the signals are pol-mux signals. Different from the previous methods to conduct the ADTP-based analysis, we propose to include the (a_{ni}, b_{ni}) (i = x,y) generated ADTPs in the analysis to increase the recognition accuracy. Therefore, each signal will have three ADTPs which are generated by (a_{nx}, b_{nx}), (a_{ny}, b_{ny}) and (c_{n}, d_{n}).

With the above mentioned ADTPs, PCA and ANN are combined for modulation format/bit rate recognition. The schematic is shown in Fig. 2.

OSA CONTINUUM

In the proposed new method, the PCA step is applied to the raw data and it achieves two goals: to generate the weight vector library for ANN training and to generate the weight vectors for the signals to be recognized.

The weight vector library generation in the PCA step is as follows. As discussed above, the training signals are used to generate the ADTPs, obtaining three ADTPs per training signal. The ADTPs are used to create a matrix $\mathbf{X}$

$$\mathbf{X} = [x_1, x_2, \ldots, x_M] \tag{2}$$

where $\boldsymbol{x}_{\mathrm{i}}$ is a vector generated from the three ADTPs of a training signal. It is generated by piling up the rows of three N×N ADTP matrices into a vector with $3\mathrm{N}^2$ elements. In our case, N is chosen to be 32. The total number of vectors is M, which is determined by the size of the library for the pre-stored training signals before the data recognition. The larger the data base is, the more accurate the recognition will be. The matrix $\mathbf{X}$ is processed to generate a matrix $\mathbf{C}$ before being sent for further analysis [13]:

$$\begin{aligned} \mathbf{C} &= \mathbf{Y}\mathbf{Y}^T \\ \mathbf{Y} &= [x_1 - \psi, x_2 - \psi, \ldots, x_M - \psi] \\ \psi &= \frac{1}{M}\sum_{i=1}^{M} x_i \end{aligned} \tag{3}$$

The matrix $\mathbf{C}$ will be analyzed by evaluating its eigenvalues and eigenvectors. The principal eigenvalues λ_{k} are selected and the corresponding principal eigenvectors $\boldsymbol{v}_{\mathrm{k}}$ are collected. The principal eigenvalues λ_{k} are defined as the eigenvalues whose sum accounts for a significant proportion of the sum of all eigenvalues. Usually, the proportion to determine the principal eigenvalues is 90% or more [13]. In our case, it is 99%. The principal eigenvectors $\boldsymbol{v}_{\mathrm{k}}$ are orthogonal to each other.

With the principal eigenvectors, the signal vector $\boldsymbol{x}_{\mathrm{i}}$ can be projected onto the corresponding PCA component directions by taking the inner product [13]

$$\begin{aligned} w^i{}_k &= x_i{}^T v_k \\ k &= 1 \cdots K \end{aligned} \tag{4}$$

where K is the number of the selected principal vectors. Hence, we are able to build up a PCA weight vector library comprised of the vector $\mathbf{w}^i$ with

$$\mathbf{w}^i = (w^i{}_1, w^i{}_2 \cdots w^i{}_K) \tag{5}$$

The weight vector library will be sent to train the weight coefficients and the bias coefficients of the ANN.

During the signal recognition stage, the detected signal will also be polarization splitted and then three ADTPs will be generated. The ADTPs will form a vector z with $3N^2$ elements, which will be projected onto the space spanned by K principal eigenvectors. Similarly, the inner product between the signal vector z and the principal eigenvectors generates a set of coefficients, $\mathbf{q} = [\mathrm{q}_1, \ldots \mathrm{q}_{\mathrm{K}}]$.

In the existing literatures [13–14], the Euclidean distance between $\mathbf{q}$ and the weight vectors in the PCA weight vector library is used to determine the signal type. In this work, we propose to use an ANN to achieve signal classification, i.e., $\mathbf{q}$ will be sent to the ANN to determine the signal modulation format/bit rate.

The ANN relies on the neuron nodes to mimic different linear and nonlinear functions, and its basic structure is shown in Fig. 3 [18]. The network consists of three layers, namely the input

OSA CONTINUUM

layer, the hidden layer and the output layer. The input layer has the same neuron number as that of the principal eigenvectors, i.e. K. The hidden layer has N_h neurons, which can be adjusted according to the requirements. The number of neurons of the output layer, namely N_o, is equal to the number of signal types, which is 16 in our case. The transfer function for the hidden layer $f(x)$ is the hyperbolic tangent function and the transfer function for the output layer $g(x)$ is the linear function [13], i.e.

$$f(x) = \frac{e^x - e^{-x}}{e^x + e^{-x}}$$
$$g(x) = x \tag{6}$$

As illustrated in Fig. 3, the ANN has ${W_{lj}}^{I}$ as the weights between the input layer and the hidden layer, and ${W_{jk}}^{II}$ as the weights between the hidden layer and the output layer respectively. It also has ${b_j}^{I}$ and ${b_k}^{II}$ as the biases for the hidden layer and the output layer, respectively.

The data in the weight vector library are used as the training data set for the ANN to optimize the corresponding neuron weights and biases by the backward-propagation (BP) algorithm. The target output vectors are [1 0. . . .], [0 1. . . ..], . . . , [0. . . ..1] according to the different modulation formats/bit rates. The error between the ANN output (with the training signals) and the target output is evaluated and this determines the updated values for the weights and biases. The error propagates from layers to layers and all weights and the biases in the ANN are updated accordingly. The iteration to update the weights and the biases stops when the precision limits are met. After the ANN has been trained, the detected signal weight vector **q** is sent to the ANN for modulation format/bit rate recognition. The output vector of the ANN is a vector with its number of elements equal to the number of modulation formats/bit rates. The final signal modulation format/bit rate is determined by comparing the output vector with respect to the vectors [1 0. . . .], [0 1. . . ..], . . . , [0. . . ..1].

The proposed method does have the capability to be extended to recognize modulation formats that were not trained. If an untrained modulation format is to be recognized, the output vector will have multiple large elements. This will be an indication to update the ANN architecture to adapt to more modulation formats.

3. Results and discussions

Simulations have been conducted with 16 different modulation formats/bit rates, as listed in Tables 1–3. 14 of them are the traditional modulate formats in the optical transmission systems, like OOK, QPSK, 16QAM etc. Their recognition accuracy plays the most important role in evaluating the recognition performance of the proposed method. 2 of the signals are OFDM signals with the sub-carrier number of 128. The purpose to introduce OFDM signals is to test the applicability of the method on multi-carrier signals. It is worth mentioning that same modulation format with different baud rates are treated as distinctive signal types, because they have different ADTPs as discussed before**.** The signals experience fiber dispersion and random polarization rotations. The dispersion is assumed to be partially compensated by the dispersion compensation fiber and the residual dispersion varies during the analysis. The signal ADTPs obtained with the pairs (c_n, d_n) are shown in Fig. 1. The delay ΔT is equal to 15ps.

3.1. Comparison between the proposed method and the existing methods

In the analysis, it is found that the ADTP grid to generate the histogram should be chosen carefully. In our case, it is optimized as 16×16. The signals to generate the PCA matrix **C** include 16 different modulation formats/bit rates with 5 residual dispersion values (0, 100, 200, 300, 400 ps/nm). Each modulation format/bit rate with one distinctive dispersion value have 200 signal examples, which differ in random binary sequences and fiber polarization rotation directions. Hence, the total number of examples for the PCA matrix generation is 16000. These 16000

Table 1. Signal recognition performance by PCA with the OSNR of 20dB

	10Gbps RZ OOK	10Gbps NRZ OOK	20Gbps RZ QPSK	20Gbps NRZ QPSK	20Gbps PM RZ QPSK	20Gbps PM NRZ QPSK	20Gbps RZ OOK	20Gbps NRZ OOK	40Gbps PM RZ QPSK	40Gbps PM NRZ QPSK	100Gbps PM NRZ QPSK	200Gbps PM RZ QPSK	200Gbps PM NRZ 16QAM	100Gbps PM NRZ 16QAM	200Gbps PM OFDM QPSK	200Gbps PM OFDM 16QAM
10Gbps RZ OOK	99.80%	0	0	0	0	0	0.20%	0	0	0	0	0	0	0	0	0
10Gbps NRZ OOK	0	100%	0	0	0	0	0	0	0	0	0	0	0	0	0	0
20Gbps RZ QPSK	0	0	83.60%	0	0	0	0	0	16.40%	0	0	0	0	0	0	0
20Gbps NRZ QPSK	0	0	0	99.90%	0	0	0	0	0	0.10%	0	0	0	0	0	0
20Gbps PM RZ QPSK	0	0	0	0	100%	0	0	0	0	0	0	0	0	0	0	0
20Gbps PM NRZ QPSK	0	0	0	0	0	100%	0	0	0	0	0	0	0	0	0	0
20Gbps RZ OOK	0.15%	0	0	0	0	0	99.85%	0	0	0	0	0	0	0	0	0
20Gbps NRZ OOK	0	0.03%	0	0	0	0	0	99.98%	0	0	0	0	0	0	0	0
40Gbps PM RZ QPSK	0	0	15.83%	0	0	0	0	0	84.18%	0	0	0	0	0	0	0
40Gbps PM NRZ QPSK	0	0	0	0	0	0	0	0	0	99.98%	0.03%	0	0	0	0	0
100Gbps PM NRZ QPSK	0	0	0	0	0	0	0	0	0	0	89.08%	0	10.93%	0	0	0
200Gbps PM RZ QPSK	0	0	0	0	0	0	0	0	0	0	0	81.95%	0	0	8.63%	9.43%
200Gbps PM NRZ 16QAM	0	0	0	0	0	0	0	0	0	0	11.60%	0	88.35%	0	0.03%	0.03%
100Gbps PM NRZ 16QAM	0	0	0	0	0	0	0	0	0	0	0	0	0	100%	0	0
200Gbps PM OFDM QPSK	0	0	0	0	0	0	0	0	0	0	0	7.93%	0	0	75.65%	16.43%
200Gbps PM OFDM 16QAM	0	0	0	0	0	0	0	0	0	0	0	2.00%	0	0	3.40%	94.60%

Table 2. Signal recognition performance by ANN with the OSNR of 20dB

	10Gbps RZ OOK	10Gbps NRZ OOK	20Gbps RZ QPSK	20Gbps NRZ QPSK	20Gbps PM RZ QPSK	20Gbps PM NRZ QPSK	20Gbps RZ OOK	20Gbps NRZ OOK	40Gbps PM RZ QPSK	40Gbps PM NRZ QPSK	100Gbps PM NRZ QPSK	200Gbps PM RZ QPSK	200Gbps PM NRZ 16QAM	100Gbps PM NRZ 16QAM	200Gbps PM OFDM QPSK	200Gbps PM OFDM 16QAM
10Gbps RZ OOK	100%	0	0	0	0	0	0	0	0	0	0	0	0	0	0	0
10Gbps NRZ OOK	0	99.63%	0	0.05%	0	0	0	0.33%	0	0	0	0	0	0	0	0
20Gbps RZ QPSK	0.15%	0	70.05%	0	0.03%	0	0	0.80%	28.95%	0	0.03%	0	0	0	0	0
20Gbps NRZ QPSK	0	0	0	99.80%	0	0	0	0	0	0	0	0	0	0.20%	0	0
20Gbps PM RZ QPSK	0.03%	0	0	0	99.95%	0	0	0.03%	0	0	0	0	0	0	0	0
20Gbps PM NRZ QPSK	0	0	0	0	0	100%	0	0	0	0	0	0	0	0	0	0
20Gbps RZ OOK	0.98%	0	0	0	0.43%	0	98.53%	0	0	0	0	0	0	0	0.05%	0.03%
20Gbps NRZ OOK	0	0.03%	0	0	0.83%	0	0.03%	99.00%	0	0	0	0	0	0	0.13%	0
40Gbps PM RZ QPSK	0	0	19.93%	0.23%	0.03%	0	0.03%	0.13%	75.80%	0	3.80%	0	0.05%	0	0.03%	0
40Gbps PM NRZ QPSK	0	0	0	0	0	0	0	0	0	99.93%	0	0	0	0.08%	0	0
100Gbps PM NRZ QPSK	0.03%	0	0	0	0.03%	0	0	0	0	0	81.70%	0	18.25%	0	0	0
200Gbps PM RZ QPSK	0	0	0	0	0	0	0.55%	0	0	0	0	88.90%	0	0	9.95%	0.60%
200Gbps PM NRZ 16QAM	0	0	0	0	0.08%	0.03%	0.03%	0	0	0	2.03%	0	97.83%	0	0.03%	0
100Gbps PM NRZ 16QAM	0	0	0	0	0	0	0	0	0	0	0	0	0	100%	0	0
200Gbps PM OFDM QPSK	0	0	0	0	0	0	0.10%	0	0	0	0	13.75%	0	0	82.63%	3.53%
200Gbps PM OFDM 16QAM	0	0	0	0	0.08%	0	1.08%	0	0	0	0	24.65%	3.55%	0	17.95%	52.70%

Table 3. Signal recognition performance by PCA+ANN with the OSNR of 20dB

	10Gbps RZ OOK	10Gbps NRZ OOK	20Gbps RZ QPSK	20Gbps NRZ QPSK	20Gbps PM RZ QPSK	20Gbps PM NRZ QPSK	20Gbps RZ OOK	20Gbps NRZ OOK	40Gbps PM RZ QPSK	40Gbps PM NRZ QPSK	100Gbps PM NRZ QPSK	200Gbps PM RZ QPSK	200Gbps PM NRZ 16QAM	100Gbps PM NRZ 16QAM	200Gbps PM OFDM QPSK	200Gbps PM OFDM 16QAM
10Gbps RZ OOK	99.63%	0	0	0	0	0	0.38%	0	0	0	0	0	0	0	0	0
10Gbps NRZ OOK	0	99.98%	0	0	0	0	0	0.03%	0	0	0	0	0	0	0	0
20Gbps RZ QPSK	0	0	99.08%	0	0	0	0	0	0.90%	0	0	0	0.03%	0	0	0
20Gbps NRZ QPSK	0	0	0	99.88%	0	0	0	0	0	0.03%	0	0	0	0.10%	0	0
20Gbps PM RZ QPSK	0	0	0	0	99.90%	0	0.001	0	0	0	0	0	0	0	0	0
20Gbps PM NRZ QPSK	0	0	0	0	0	99.98%	0	0	0	0	0	0	0	0.03%	0	0
20Gbps RZ OOK	0.25%	0	0	0	0	0	99.75%	0	0	0	0	0	0	0	0	0
20Gbps NRZ OOK	0	0	0	0	0	0	0	100%	0	0	0	0	0	0	0	0
40Gbps PM RZ QPSK	0	0	0.58%	0	0	0	0	0	99.43%	0	0	0	0	0	0	0
40Gbps PM NRZ QPSK	0	0	0	0	0	0	0	0	0	99.98%	0	0	0	0.03%	0	0
100Gbps PM NRZ QPSK	0	0	0	0	0	0	0	0	0	0	94.30%	0	5.70%	0	0	0
200Gbps PM RZ QPSK	0	0	0	0	0	0	0	0	0	0	0	97.65%	0	0	1.63%	0.73%
200Gbps PM NRZ 16QAM	0	0	0	0	0	0	0	0	0	0	1.80%	0	97.88%	0.28%	0	0.05%
100Gbps PM NRZ 16QAM	0	0	0	0	0	0	0	0	0	0	0%	0	0	100%	0	0
200Gbps PM OFDM QPSK	0	0	0	0	0.10%	0	0	0	0.13%	0	0	2.23%	0	0	88.10%	9.45%
200Gbps PM OFDM 16QAM	0	0	0	0	0	0	0	0	0	0	0	3.55%	0.33%	0	14.85%	81.30%

OSA CONTINUUM

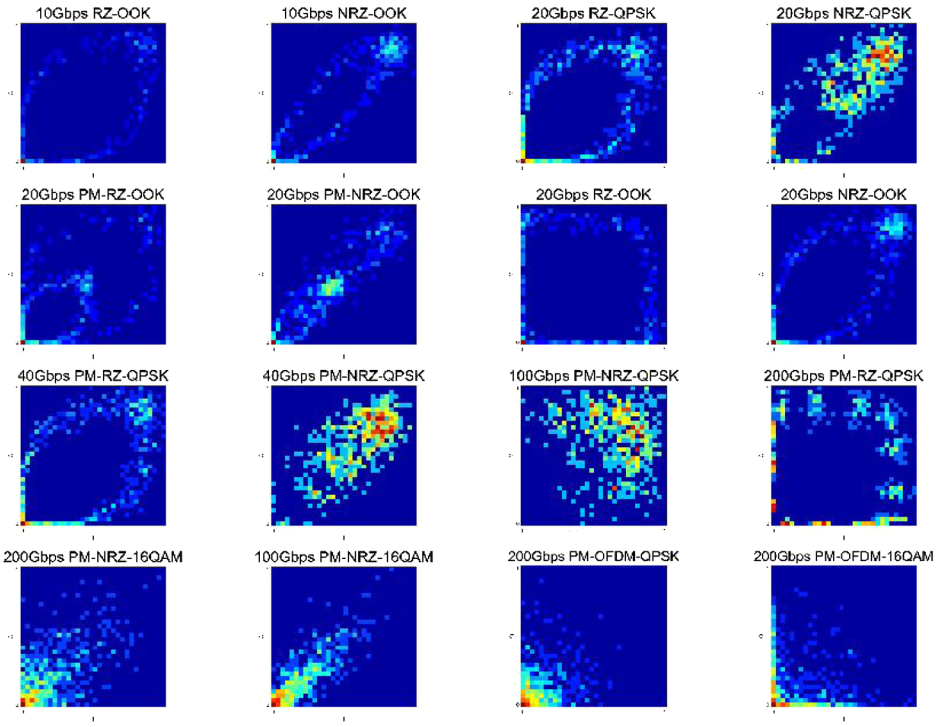

Fig. 1. The generated ADTPs by the pair (c_n, d_n) with different modulation formats and data bit rates.

examples are also converted into 16000 PCA weight vectors, which are used to train the ANN to get ready for the recognition of the detected signals. The detected signals which are used to evaluate the recognition performance include 800 examples for each modulation format/bit rate and each distinctive residual dispersion value. The total number of examples for test is 64000. The ANN has the input nodes equal to the number of the principal vectors, 20 nodes for the hidden layer, and 16 nodes for the output layer.

Firstly, the OSNR is assumed to be 20 dB. The results of the proposed method are listed in Table 3. For comparison, the results by the pure PCA [13] and the pure ANN [15] are listed in Table 1 and Table 2, respectively. From Tables 1–3, it can be seen that the proposed method significantly improves the recognition performance in comparison with the existing methods, i.e. PCA in [13] and ANN in [15].

Considering the traditional 14 signals, the total recognition accuracies are 94.76%, 93.65% and 99.10% by the pure PCA, the pure ANN, and the PCA + ANN approaches (the rates are the combination of the rates for all of the 5 residual CD values). For the PCA case, the most significant error (about 16%) occurs when distinguishing 20Gbps RZ QPSK and 40Gbps PM-RZ-QPSK signals, as well as 100Gbps PM-NRZ-QPSK and 200Gbps NRZ-16QAM signals (about 10%). For the ANN case, high recognition error (about 30% and 20%) also occurs for these two groups of modulation formats/bit rates. This indicates that it is very difficult to recognize these two groups. This can also be seen from the ADTPs in Fig. 1, which look quite alike for the two above-mentioned groups of modulation formats/bit rates. However, the proposed PCA + ANN method can distinguish these two groups of modulation formats/bit rates with less than 0.01% and 6% recognition error rates. For the two OFDM signals, the proposed method can achieve about 85% recognition accuracy, which improves in comparison with the pure ANN methods (about 70%) and it is comparable with the pure PCA method (about 85%). Most of the misrecognition

OSA CONTINUUM

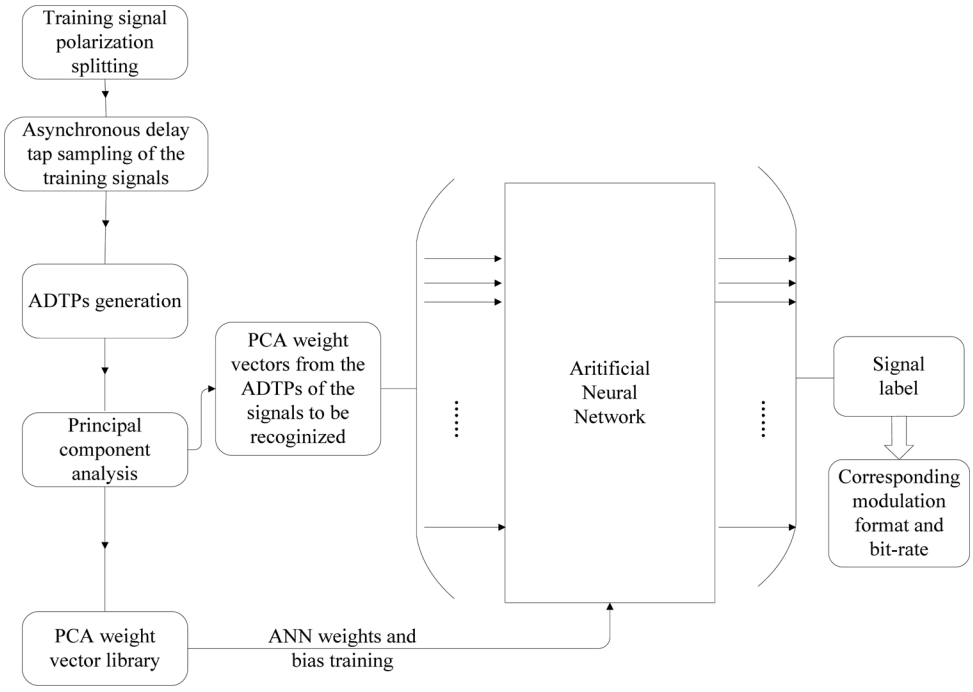

Fig. 2. The schematic of PCA & ANN-based recognition method.

occurs between the two OFDM signals. In order to further improve the recognition accuracy for the OFDM signals, one may consider implementing the convolutional neural network (CNN) instead of the ANN used in this work.

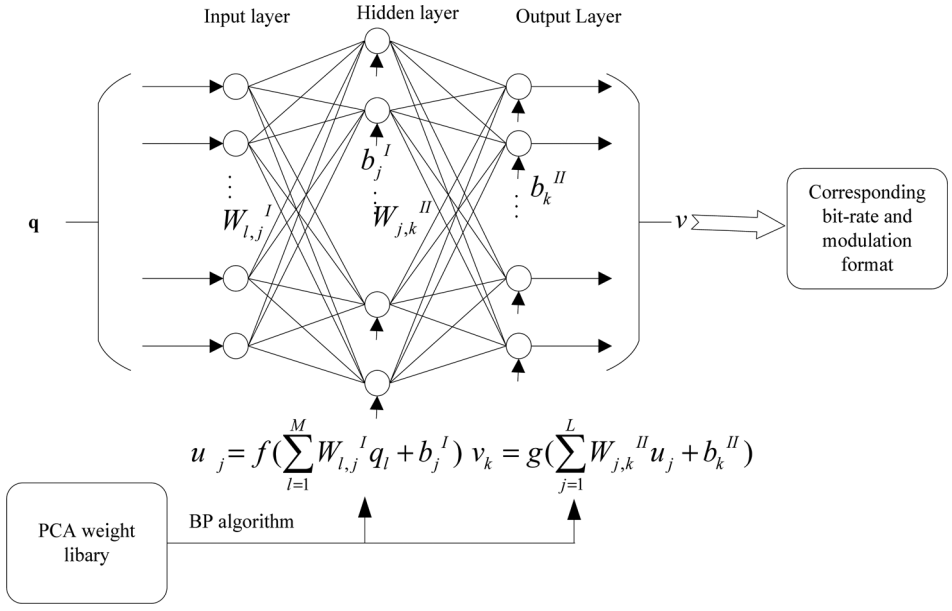

Fig. 3. The schematic of the ANN structure used in this work

OSA CONTINUUM

The results in Table 3 also indicate that the method is quite resilient to the residual chromatic dispersion. In order to demonstrate this more clearly, the recognition error rates under different residual CD values are shown in Fig. 4. It can be concluded from the figure that although residual CD can reduce the recognition accuracy, it maintains at an acceptable level until the residual CD reaches 400 ps/nm. If the residual CD further increases to 500ps/nm and 600ps/nm, the overall recognition accuracies reduce quite significantly to about 80% and 75% respectively. Therefore, the proposed method should be used together with a tunable dispersion compensator to ensure that the residual CD is within a reasonable range if it is to be implemented in a dispersion un-compensated link. The proposed method is also robust with respect to different OSNRs. When the OSNR varies to 10 dB and 15 dB, very good performance has been observed as well. The results shown in Fig. 5 demonstrate that the OSNR variations do impact the performance of the proposed method, but also at an acceptable level. For 20 dB to 15 dB, the degradation is quite minor. Even if the OSNR degrades to 10 dB, the recognition accuracies of most of the signals degrade less than 2%. The worst degradation is for the 100Gbps PM-NRZ-QPSK, which is about 15% in comparison with that of the 20 dB case.

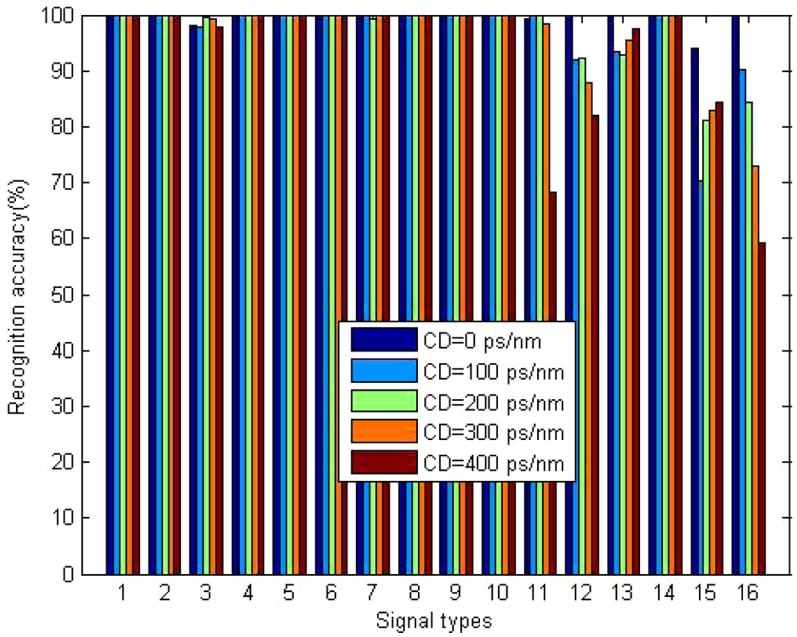

Fig. 4. Recognition accuracy for 16 modulation formats/bit rates with the proposed method with the residual CD as 0, 100, 200, 300, and 400 ps/nm.

3.2. System-level verification of the proposed method

In the system simulation setup, a 1000 km long fiber is divided into 20 spans and each span has an optical amplifier to combat the span loss. The fiber has the dispersion of -20 ps^2/km and the polarization mode dispersion (PMD) of 0.1 ps/sqrt(km). During the simulation, the fiber is divided into many short sections and the signals undergo random rotations and experience polarization mode dispersion. Fiber nonlinearity is not included, because it is computational intensive to include its impact via the split step Fourier method (SSFM) as it requires numerous rounds of discrete Fourier transform (DFT) during the calculation. Fortunately, the nonlinear noise behaves as the Gaussian noise [19], and its contribution can be included in the ASE noise, which is added to each span within the transmission link. One may tune the OSNR to include the nonlinear impairments. Totally 16 modulation formats/bit rates are used for the recognition and

OSA CONTINUUM

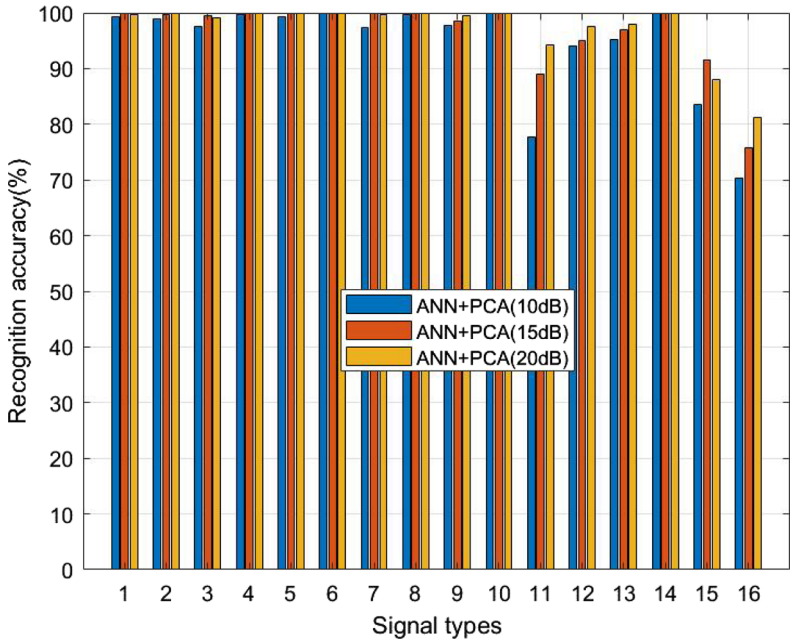

Fig. 5. Recognition accuracy for 16 modulation formats/bit rates with the proposed method under the OSNRs of 10 dB, 15 dB and 20 dB.

dispersion is compensated either by the dispersion compensation fiber or the tunable dispersion compensator at the receiver side. The residual dispersion is assumed to be 0-400 ps/nm. The simulation schematic is shown in the following Fig. 6 and the recognition results are summarized in Table 4.

From Table 4, it can be seen that the proposed method maintains very high recognition accuracy in the fiber link with the presence of PMD. For the 14 traditional signal modulate formats, the total recognition accuracy is 98.91%, which only slightly drops from 99.10% for the non-PMD case in the previous section (the rates are the combination of the rates for all of the 5 residual CD values). For the two OFDM signals, the recognition accuracy drops from 85% to 82%. This indicates that the proposed method is quite robust with respect to the PMD penalty, particularly for the traditional modulate formats.

Figures 7 and 8 show the recognition accuracy with different residual CD or under different OSNRs after the signals have been transmitted in the fiber link. Reasonable degradation has been observed if the impairments like the residual CD and the degraded OSNR have been introduced. If the residual CD is less than 300 ps/nm and the OSNR is higher than 15 dB,

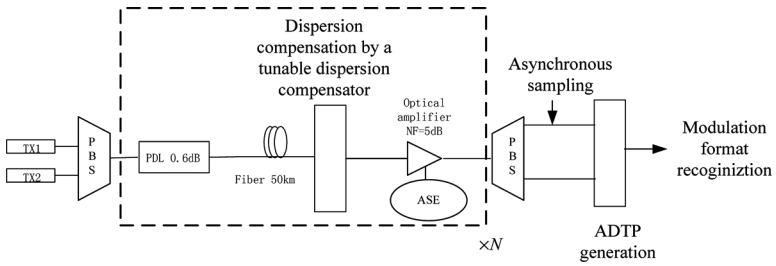

Fig. 6. The optical schematic of the transmission link

Table 4. Signal recognition performance for the signals after 1000km transmission by PCA+ANN with the OSNR of 20dB

	10Gbps RZ OOK	10Gbps NRZ OOK	20Gbps RZ QPSK	20Gbps NRZ QPSK	20Gbps PM RZ QPSK	20Gbps PM NRZ QPSK	20Gbps RZ OOK	20Gbps NRZ OOK	40Gbps PM RZ QPSK	40Gbps PM NRZ QPSK	100Gbps PM NRZ QPSK	200Gbps PM RZ QPSK	200Gbps PM NRZ 16QAM	100Gbps PM NRZ 16QAM	200Gbps PM OFDM QPSK	200Gbps PM OFDM 16QAM
10Gbps RZ OOK	100%	0	0	0	0	0	0	0	0	0	0	0	0	0	0	0
10Gbps NRZ OOK	0	100%	0	0	0	0	0	0	0	0	0	0	0	0	0	0
20Gbps RZ QPSK	0	0	99.60%	0	0	0	0	0	0.40%	0	0	0	0	0	0	0
20Gbps NRZ QPSK	0	0	0	99.90%	0	0	0	0	0	0	0	0	0	0.10%	0	0
20Gbps PM RZ QPSK	0	0	0	0	98.80%	0	0	0	0	0	0	0	1.10%	0.10%	0	0
20Gbps PM NRZ QPSK	0	0	0	0	0	100%	0	0	0	0	0	0	0	0	0	0
20Gbps RZ OOK	0	0	0	0	0	0	100%	0	0	0	0	0	0	0	0	0
20Gbps NRZ OOK	0	0	0	0	0	0	0	100%	0	0	0	0	0	0	0	0
40Gbps PM RZ QPSK	0	0	0.20%	0	0	0	0	0	99.80%	0	0	0	0	0	0	0
40Gbps PM NRZ QPSK	0	0	0	0	0	0	0	0	0	100%	0	0	0	0	0	0
100Gbps PM NRZ QPSK	0	0	0	0	0	0	0	0	0	0	93.50%	0	6.50%	0	0	0
200Gbps PM RZ QPSK	0	0	0	0	0	0	0	0	0	0	1.00%	94.70%	0	0	2.70%	1.60%
200Gbps PM NRZ 16QAM	0	0	0	0	0	0	0	0	0	0	1.60%	0	98.40%	0	0	0
100Gbps PM NRZ 16QAM	0	0	0	0	0	0	0	0	0	0	0	0	0	100%	0	0
200Gbps PM OFDM QPSK	0	0	0	0	0.10%	0	0	0	0	0	0	1.10%	0	0	87.40%	11.40%
200Gbps PM OFDM 16QAM	0	0	0	0	0	0	0	0	0	0	0	5.50%	0.10%	0	17.80%	76.60%

OSA CONTINUUM

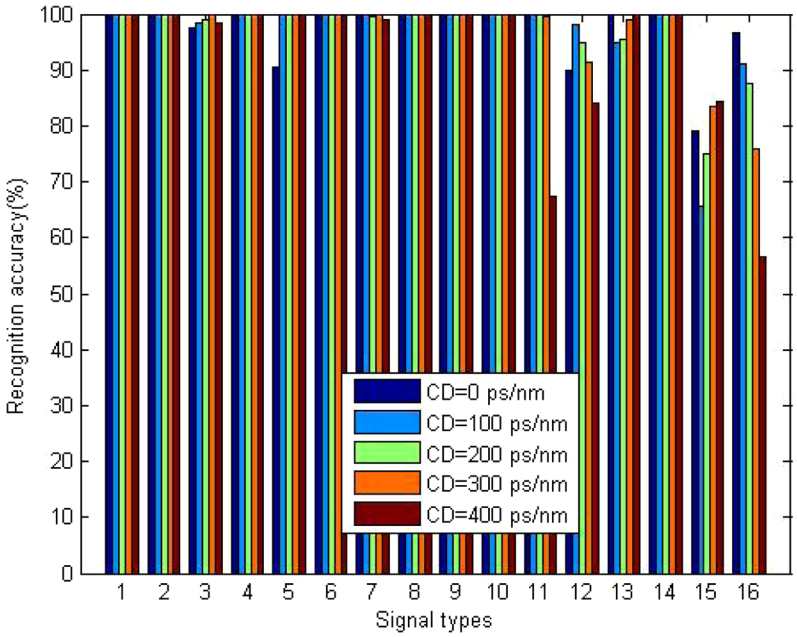

Fig. 7. Recognition accuracy for 16 modulation formats/bit rates after transmission in a 1000 km long fiber link with the proposed method with the residual CD as 0, 100, 200, 300, and 400 ps/nm.

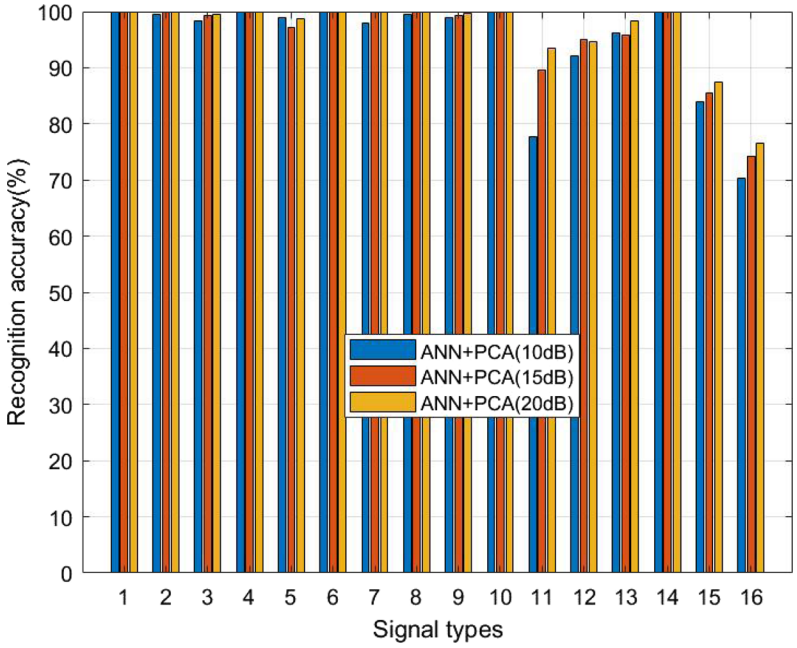

Fig. 8. Recognition accuracy for 16 modulation formats/bit rates after transmission in a 1000 km long fiber link with the proposed method under the OSNRs of 10 dB, 15 dB and 20 dB.

the performance degradation is quite insignificant. Therefore, the proposed method maintains acceptable recognition accuracy despite the residual CD and the degraded OSNRs.

OSA CONTINUUM

4. Summary

We have proposed a novel method to distinguish modulation formats/bit rates for optical communication systems. The method splits the signal into the x and y polarizations, and three ADTPs are generated. The ADTPs are converted into a vector and the vectors formed by different training signals are used to generate a matrix to be processed by PCA to obtain the principal components. The vectors are projected onto these principal components to generate the weight vectors. The training signal generated weight vectors are sent to train an ANN, and the weight vectors generated by the detected signals will be the inputs of the ANN. The ANN outputs indicate the modulation formats/bit rates. The novel method achieves significant improvement in comparison with the existing methods. Even compared with the coherent data aided approaches, the proposed method shows advanced performance in terms of the number of modulation formats/bit rates and the identification accuracy (e.g. Reference [12]). It is worth mentioning that the proposed method (PCA + ANN) can be implemented in the coherent receivers and it can be combined with other signal processing techniques, such as the fractal dimension based method [12] to further improve the performance. Therefore, future heterogeneous optical network development could be benefited from our proposal.

Funding

National Natural Science Foundation of China (NSFC) (61775168); Natural Science Foundation of Shanghai (16ZR1438600).

References

1. T. Mizuochi, K. Ishida, T. Kobayashi, J. Abe, K. Kinjo, K. Motoshima, and K. Kasahara, "A Comparative Study of DPSK and OOK WDM Transmission Over Transoceanic Distances and Their Performance Degradations Due to Nonlinear Phase Noise," J. Lightwave Technol. **21**(9), 1933–1943 (2003).
2. A. J. Stark, Y.-T. Hsueh, T. F. Detwiler, M. M. Filer, S. Tibuleac, and S. E. Ralph, "System Performance Prediction With the Gaussian Noise Model in 100G PDM-QPSK Coherent Optical Networks," J. Lightwave Technol. **31**(21), 3352–3360 (2013).
3. Y. R. Zhou, K. Smith, R. Payne, A. Lord, L. Raddatz, M. Bertolini, T. Van De Velde, C. Colombo, E. Korkmaz, M. Fontana, and S. Evans, "1.4 Tb Real-Time Alien Superchannel Transport Demonstration Over 410 km Installed Fiber Link Using Software Reconfigurable DP-16 QAM/QPSK," J. Lightwave Technol. **33**(3), 639–644 (2015).
4. N. Guerrero Gonzalez, *et al.*, "Cognitive digital receiver for burst mode phase modulated radio over fiber links," in *36th European Conference and Exhibition on Optical Communication (ECOC) 2010*, Proc. ECOC'10, paper P6.11.
5. M. Zaerin and B. Seyfe, "Multiuser modulation classification based on cumulants in additive white Gaussian noise channel," IET Signal Process **6**(9), 815–823 (2012).
6. J. Liu, Z. Dong, K. Zhong, A. P. T. Lau, C. Lu, and Y. Lu, "Modulation format identification based on received signal power distributions for digital coherent receivers," in *Optical Fiber Communication Conference*, OSA Technical Digest (online) (Optical Society of America, 2014), paper Th4D.3.
7. S. M. Bilal, G. Bosco, Z. Dong, A. P. Tao Lau, and C. Lu, "Blind modulation format identification for digital coherent receivers," Opt. Express **23**(20), 26769–26778 (2015).
8. R. Borkowski, D. Zibar, A. Caballero, V. Arlunno, and I. T. Monroy, "Optical Modulation Format Recognition in Stokes Space for Digital Coherent Receivers," in *Optical Fiber Communication Conference/National Fiber Optic Engineers Conference 2013*, OSA Technical Digest (online) (Optical Society of America, 2013), paper OTh3B.3.
9. R. Boada, R. Borkowski, and I. T. Monroy, "Clustering algorithms for Stokes space modulation format recognition," Opt. Express **23**(12), 15521–15531 (2015).
10. M. Xiang, Q. Zhuge, M. Qiu, X. Zhou, F. Zhang, M. Tang, D. Liu, S. Fu, and D. V. Plant, "Modulation format identification aided hitless flexible coherent transceiver," Opt. Express **24**(14), 15642–15655 (2016).
11. S. Fu, Z. Xu, J. Lu, H. Jiang, Q. Wu, Z. Hu, M. Tang, D. Liu, and C. C.-K. Chan, "Modulation format identification enabled by the digital frequency-offset loading technique for hitless coherent transceiver," Opt. Express **26**(6), 7288–7296 (2018).
12. H. Zhou, M. Tang, X. Chen, Z. Feng, Q. Wu, S. Fu, and D. Liu, "Fractal dimension aided modulation formats identification based on support vector machines," in *43th European Conference and Exhibition on Optical Communication (ECOC) 2017*, Proc. ECOC'17, pp. 1–3.
13. M. C. Tan, F. N. Khan, W. H. Al-Arashi, Y. Zhou, and A. P. Tao Lau, "Simultaneous Optical Performance Monitoring and Modulation Format/Bit-Rate Identification Using Principal Component Analysis," J. Opt. Commun. Netw. **6**(5), 441–448 (2014).

OSA CONTINUUM

14. F. N. Khan, Y. Yu, M. C. Tan, W. H. Al-Arashi, C. Yu, A. P. Tao Lau, and C. Lu, "Experimental demonstration of joint OSNR monitoring and modulation format identification using asynchronous single channel sampling," Opt. Express **23**(23), 30337–30346 (2015).
15. F. N. Khan, Y. Zhou, A. P. Tao Lau, and C. Lu, "Modulation format identification in heterogeneous fiber-optic networks using artificial neural networks," Opt. Express **20**(11), 12422–12431 (2012).
16. L. Guesmi, A. M. Ragheb, H. Fathallah, and M. Menif, "Experimental Demonstration of Simultaneous Modulation Format/Symbol Rate Identification and Optical Performance Monitoring for Coherent Optical Systems," J. Lightwave Technol. **36**(11), 2230–2239 (2018).
17. B. Kozicki, A. Maruta, and K.-i. Kitayama, "Transparent performance monitoring of RZ-DQPSK systems employing delay-tap sampling," J. Opt. Netw. **6**(11), 1257–1269 (2007).
18. The MathWorks, Inc., *Neural Network Toolbox User's Guide version 4* (2004).
19. P. Poggiolini, G. Bosco, A. Carena, V. Curri, Y. Jiang, and F. Forghieri, "The GN-Model of Fiber Non-Linear Propagation and its Applications," J. Lightwave Technol. **32**(4), 694–721 (2014).